Materials Science and Engineering A 395 (2005) 295–300

MATERIALS SCIENCE & ENGINEERING A

www.elsevier.com/locate/msea

Instrumented microindentation studies on long-term aged materials: work-hardening exponent and yield ratio as new degradation indicators

Jae-il Jang[a,*], Yeol Choi[a,b], Yun-Hee Lee[b], Dongil Kwon[b]

[a] *Frontics Inc., Research Institute of Advanced Materials, Seoul National University, Seoul 151-742, South Korea*
[b] *School of Materials Science and Engineering, Seoul National University, Seoul 151-742, South Korea*

Received 29 September 2004; accepted 22 December 2004

Abstract

Using an instrumented microindentation technique for evaluating tensile properties, the present study was undertaken to determine new mechanical parameters measurable in the field that can indicate time-dependent material degradation. Lab-scale tests performed on a Cr–Ni steel and a Cr–Mo steel, two of the most popular heat-resistant steels for facilities in petrochemical and power plants, showed that the work-hardening exponent and yield ratio could be useful as mechanical parameters indicating degradation. The in-field applicability of these parameters was partly verified.

Keywords: Aging; Microindentation; Heat resistant steel; Work-hardening exponent; Yield ratio

1. Introduction

1.1. Background

Industries have always wanted to operate their high-temperature facilities safely and economically far beyond their initial design life. Meeting this demand essentially requires periodic reliability diagnoses based on quantitative evaluation of time-dependent failures, and hence many kinds of non-destructive testing (NDT) techniques have been developed. Time-dependent failures of high-temperature structures and facilities fall into three categories: (1) thickness reduction by corrosion and wear, (2) cracking damage during manufacturing or operation, and (3) mechanical property degradation allowed by easy diffusion of atoms at high temperature. Most NDT techniques (from basic visual tests to new ultrasonic tests called 'time of flight diffraction (TOFD)' tests) have focused on the evaluation of thickness reduction and cracking damage; few NDT techniques have been developed for direct measurement of mechanical property degradation, including softening/hardening and embrittlement. Standard mechanical testing methods such as uniaxial tensile and fracture mechanics tests cannot be used for in-service components because of their destructive procedures and sample size requirements. With these difficulties in direct measurement of mechanical property degradation, microstructural degradation has been evaluated for predicting mechanical-property change, and thus remaining lifetime through several NDTs such as replica analysis, electronic resistance test, ultrasonic test, and so on. Converting microstructural change to mechanical property change in this way needs a well-established database because the conversion depends very strongly on empirical relationships between microstructure and mechanical properties.

To overcome the limitations of conventional NDT techniques in measuring mechanical property degradation, the present study adopts an instrumented microindentation technique based on the analyzing procedure developed by Kwon and co-workers [1,2]. The technique can provide flow properties (such as flow curve, tensile strength, yield strength, and work-hardening exponent) almost non-destructively by

* Corresponding author. Present address: Department of Materials Science and Engineering, The University of Tennessee, Knoxville, TN 37996-2200, USA. Tel.: +1 865 974 8661.
E-mail addresses: jijang@frontics.com, jangj@ornl.gov (J.-i. Jang).

0921-5093/$ – see front matter
doi:10.1016/j.msea.2004.12.033

analyzing indentation load–depth curves that represent the deformation behavior of the sample beneath the rigid spherical indenter. Compared with other spherical microindentation techniques developed for the same purpose [3–6], the technique adopted here does not need the pre-determination of unknown material coefficients through preliminary tests as discussed below. Additionally, when a portable indentation system is used, as here, the technique has many advantages in in-field applications: (i) the testing procedure is very simple and does not require tedious specimen preparation and (ii) no damage remains in the structures tested. However, the utility of this technique in appraising degradation of aged materials has not yet been assessed in detail. In this work, the instrumented microindentation testing technique is used to determine the major mechanical parameters indicating degradation. First, through laboratory tests, the mechanical parameters generally useful in indicating degradation were determined. The indentation technique was then applied to in-field components to evaluate the in-field applicability of these parameters.

1.2. Instrumented microindentation technique for tensile property measurement

Fig. 1 shows a typical indentation load–depth curve obtainable during instrumented spherical indentations on steel. Unlike curves from sharp indentation using pyramidal indenter, loading curves are quite linear due to the counterbalance of spherical geometry and work hardening in tested steel. Representative stress and strain are defined in terms of measured indentation contact parameters such as contact depth (h_c), indenter shape, and the morphology of the deformed sample surface. The contact depth at maximum indentation load can be evaluated by analyzing the unloading curve using concepts of indenter geometry and elastic deflection [7]:

$$h_c^* = h_{max} - \omega(h_{max} - h_i) \quad (1)$$

where h_i is the intercept indentation depth (see Fig. 1) and the indenter shape parameter ω is 0.75 for a spherical indenter. The material pile-up around the indentation makes the actual contact radius larger than expected. The extent of this pile-up can be expressed by a constant c and the steel work-hardening exponent n [8,9]:

$$c^2 = \frac{a^2}{a^{*2}} = \frac{5(2-n)}{2(4+n)} \quad (2)$$

where a is the actual contact radius and a^* is the contact radius without the pile-up. From the geometry of the spherical indenter, the real contact radius is expressed in terms of h_c^* and indenter radius R as:

$$a^2 = \frac{5(2-n)}{2(4+n)}(2Rh_c^* - h_c^{*2}) \quad (3)$$

With these parameters, the representative stress and strain are determined as follows. The representative strain of indentation, ε_R, is evaluated from the material displacement beneath the indenter along the indentation axis direction. The strain can be expressed at the contact radius position by using a fitting constant α (taken as 0.1 for various steels [1]) as in Eq. (4):

$$\varepsilon_R = \frac{\alpha}{\sqrt{1-(a/R)^2}}\frac{a}{R} \quad (4)$$

Since the elastic and elastic/plastic deformation stages in steels generally occur at very low indentation loads, only the plastic deformation stage is considered here. The mean contact pressure (P_m), obtained by dividing maximum load (P_{max}) by the contact area (πa^2), is known to be about three times the representative stress (σ_R) for fully plastic deformation of steels [1,10,11]. When multiple loading–unloading sequences are made at one location on the target material, as shown in Fig. 2, a series of representative stress and strain values can be determined by analyzing each unloading curve according to the above procedure, then the values can be fitted as a simple power-law-type Hollomon Eq. (5) [12]:

$$\sigma = K(\varepsilon)^n \quad (5)$$

where K is the strength coefficient. The exact values of the work-hardening exponent and strength coefficient are calcu-

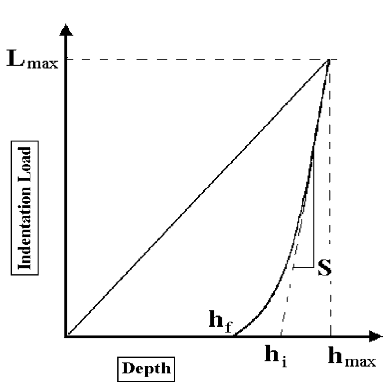

Fig. 1. Schematic diagram of typical load–depth curve obtainable during instrumented spherical indentations on steel.

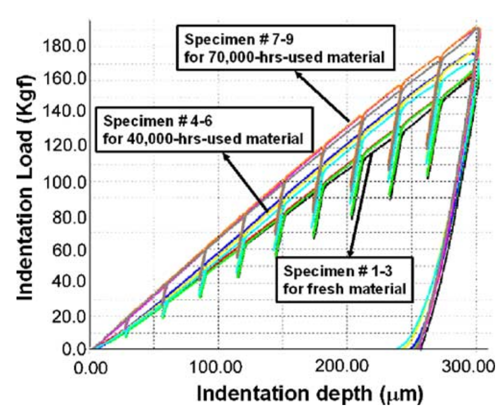

Fig. 2. Superposition of load–displacement curves obtained from multiple indentations of Cr–Ni steels.

lated by the iteration method [1]. While true stress always increases with true strain, the ultimate tensile strain can be determined using Considère's criterion [12] and the yield strength can be predicted by extrapolation of Eq. (5) to the low-strain regime. Since it is well accepted that Hollomon equation generally underestimates the stress value near the yield point (for example, see [13]), the appropriate 0.2% offset yield strength was calculated in this method by taking yield strain as 0.01 which was determined experimentally for structural steels [2]. The reliability and reproducibility of the tensile properties obtained from this testing technique are well introduced in authors' previous work [14]. In the paper [14], comparison of the tensile properties from indentation tests with those from conventional tensile tests revealed that this indentation technique could provide reproducible and reasonably precise flow properties (error range is smaller than 10%).

2. Experimental procedure

Indentation tests were performed in the laboratory and the field. To determine a useful mechanical parameter for mechanical property degradation in lab-scale tests, two representative heat-resistant steels frequently used in petrochemical and power plants were selected: a Cr–Ni-type steel (HK-40 steel) and a Cr–Mo-type steel (2.25Cr–1Mo steel); chemical compositions are listed in Table 1. Since the objective of this study is in-field applications, long-term aged samples were sought out to be used instead of the accelerated-aged samples generally used in aging studies. Thus, the Cr–Ni steels were taken from totally degraded reformer tubes of a plant in service at 1173 K for 40,000 and 70,000 h, respectively, and Cr–Mo steel samples were aged at 723 K (critical condition for operating temperatures between 643 and 723 K) for 10,000, 30,000, and 50,000 h. According to the microstructure data provided with the samples (not shown here), the Cr–Ni steels (thermally aged under stress) exhibited more extensive material degradation than the Cr–Mo steels (aged without stress); the 70,000-h-used Cr–Ni steel showed high cavity fraction (almost 1%) while the 50,000-h-aged Cr–Mo steel did not show clear microstructural degradation. This can be easily predicted since stress is known to accelerate the nucleation and growth of cavities and subgrains [15,16]. In our in-field tests for assessing the applicability of the parameters determined through lab-scale tests, five structural components made of different steels (including A335 P5, A335 P9, A335 P22, A106B, modified H50 steel) were tested nondestructively.

A portable instrumented indentation system, AIS-2000 (Frontics Inc., Seoul, South Korea), was used both in the laboratory and the field to measure the tensile properties according to the procedure described in the previous section. The radius of the spherical indenter was 500 μm and 10 loading–unloading sequences were made at 0.3 mm/min. Load–depth curves were continuously obtained during indentation and converted to true stress–true strain curves. All the indentation tests were made at room temperature, since high-temperature use of this technique for in-field structures is impractical. Fig. 2 shows examples of the load–displacement curves obtained in this study. The indentation load clearly increased with aging time at a given maximum depth (300 μm). All the mechanical values given here are averaged values from three or five testing results. Since a small sample was used in this test, the data scatter is almost negligible and good reproducibility was observed for each material, as shown in Fig. 2.

3. Results and discussion

Before doing instrumented indentation tests, micro-Vickers hardness tests were carried out for each material at a load of 1 kg. Fig. 3 shows the change in micro-Vickers hardness of the Cr–Ni and Cr–Mo steels with long-term aging time. The Cr–Mo steel increases in hardness while the hardness of Cr–Ni steel tends to decrease, both in good agreement with previous studies [16–19]. It is known that the hardness increase of Cr–Ni steel is due to the precipitation of secondary carbide in matrix and/or precipitation of intermetallic σ phase [18], and that the hardness of Cr–Mo steel can be reduced by rearrangement of dislocation structure and carbide coarsening when the steel is thermally aged in the tempering

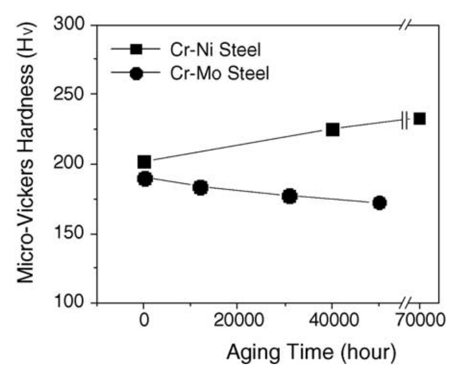

Fig. 3. Change in micro-Vickers hardness with aging time (at room temperature).

Table 1
Chemical compositions of the materials used in lab-scale tests

	C	Si	Mn	P	S	Cr	Mo	Ni	V	Fe
Cr–Ni steel	0.39	1.68	1.24	0.012	0.011	24.6	–	19.81	–	Bal.
Cr–Mo steel	0.14	0.22	0.49	0.007	0.003	2.24	0.98	–	0.02	Bal.

Bal.: balance of the composition.

temperature range (723 K in this study) [16]. However, it is interesting to note that the difference in hardness between fresh and aged material is not so large even for the 70,000-h-old Cr–Ni steel taken from the fully degraded reformer tube, i.e., hardness is not as sensitive to material degradation as had been thought. It was therefore concluded that hardness might be not an appropriate indicator of degradation, although hardness tests using portable equipment have been a very popular non-destructive technique for measuring mechanical properties in the field.

Fig. 4 shows the effects of aging on the yield strength and ultimate tensile strength obtained from the indentation tests. The yield and ultimate tensile strengths showed greater change than the hardness, that is, those strengths can be more sensitive to material degradation. While the yield strengths of both materials increase with aging time because of the increase in carbide fractions, the ultimate tensile strengths show different behavior: values for Cr–Ni steel contain a peak and those for Cr–Mo steel show a continuous decrease. The peaking behavior of the HK-40 steel has also been observed in previous research [19]. The difference between fresh material and degraded material is greater for Cr–Ni steel than Cr–Mo steel, in good agreement with the observed degree of microstructural degradation. However, the tensile strength seems inappropriate as a general degradation indicator because, like the change in hardness, the extensively degraded material sometimes has lower values (in Cr–Ni steel) and at other times higher values (in Cr–Mo steel) than fresh materials. Also, the peaking behavior, possibly caused by the reason discussed below, makes predicting the aging effect

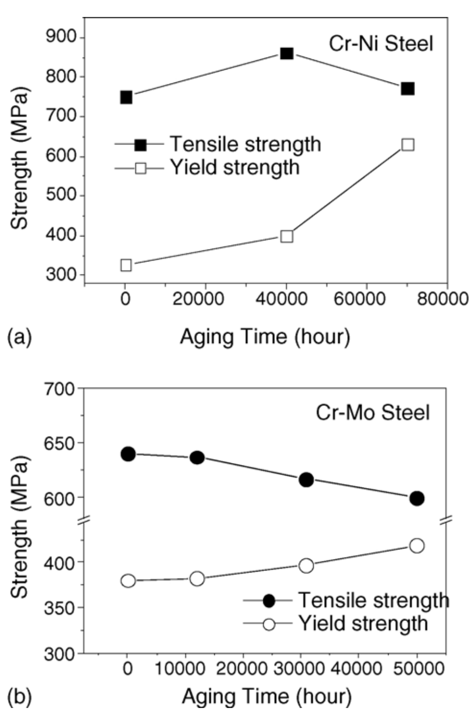

Fig. 4. Variations in tensile and yield strength with increasing aging time (at room temperature): (a) Cr–Ni steel and (b) Cr–Mo steel.

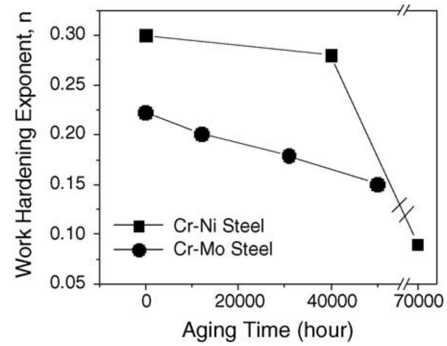

Fig. 5. Change in work-hardening exponent with aging time (at room temperature).

more difficult. On the other hand, the yield strength also has some limitations for use as an indicator, since it cannot reflect post-yielding deformation, which is more important in the fracture performance of current structural steels than the yielding phenomenon itself.

As a next step towards finding another candidate for general degradation indicator, the variation in the work-hardening exponent was examined. As shown in Fig. 5, the work-hardening exponent continuously decreases with aging time in both materials. It is noteworthy that the decrease is larger in Cr–Ni steel than in Cr–Mo steel, in agreement with the observed difference in microstructural degradation between the two materials. The change in work-hardening exponent can also explain the different trends in tensile strength change of the two materials. Comparison of Figs. 4 and 5 shows that abrupt decrease in the exponent of Cr–Ni steel may be attributable to the plateau observed in tensile strength change, and this is not seen in Cr–Mo steel because the tendency of the exponent to decrease is not so great. The above results suggest that the work-hardening exponent can be more useful in indicating material degradation than hardness or strength. Additionally, the absolute value of the exponent itself is a meaningful parameter in structural integrity assessment. As a material degrades, it simultaneously experiences changes in both strength characteristics (such as softening and hardening) and fracture characteristics (such as embrittlement). Unlike yield/tensile strength and hardness, which can show only the strength changes, the work-hardening exponent can be also analyzed as a parameter of embrittlement, since the exponent can be approximately equal to uniform elongation corresponding to ultimate tensile strength in materials experiencing Hollomon-equation-type plastic deformation [12]. When large plastic deformation occurs in a structural component, a decrease in the work-hardening exponent can induce severe local deformation concentration and can lessen the structure's ability to absorb the deformation by redistributing moment, which can be very harmful to structural integrity.

A difficulty arises, however, in using the work-hardening exponent in the field because the exponent value for the fresh material is often absent from material specification records,

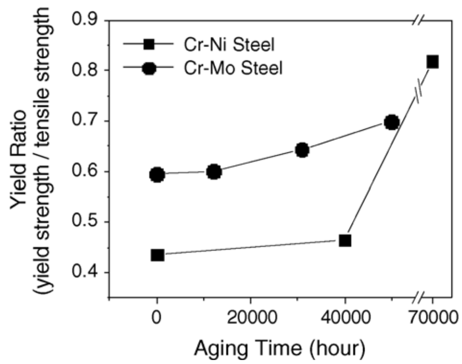

Fig. 6. Change in yield ratio with increasing aging time.

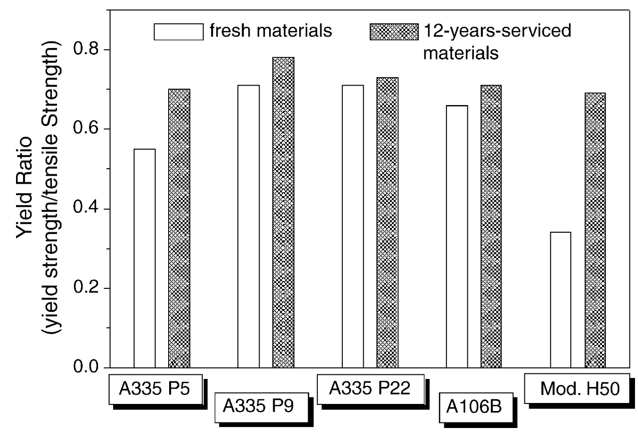

Fig. 7. Comparison of yield ratio between new materials and 12-year-serviced materials.

it is difficult to assess how much it has degraded from the fresh material. With this in mind, the authors looked for an alternative parameter that can also be obtained in the field by the indentation technique and suggested the yield-strength-to-tensile-strength ratio, the so-called yield ratio (YR), as another measure of deformability and embrittlement. As noted by Toyoda in his review article [20], the YR of a structural steel is expected to have inverse relationship with the steel's uniform elongation (i.e., a structural steel having higher YR shows lower uniform elongation). Note that the uniform elongation is theoretically the same with the work-hardening exponent according to Considère's criterion [12]. Fig. 6 shows the variation in YR with aging time. As expected, the change in YR has a trend opposite to the work-hardening exponent and it also increases by an amount similar to the decrease in the work-hardening exponent, i.e., YR can also show high sensitivity to material degradation. It should be kept in mind that YR and the work-hardening exponent can be controlled independently by recent advances in steel-making technology. Generally, however, for materials with low work-hardening exponents, YR shows a good inverse-relationship to the work-hardening exponent.

Finally, to assess the in-field applicability of the parameters proposed through the lab-scale tests, in-field indentation tests were carried out for five components made of different steels that had been used for 12 years in petrochemical power plant. Since no work-hardening exponent values had been recorded for the fresh materials, only yield ratio values were predicted for those materials after evaluating yield and tensile strength, and thus the values were compared with those of fresh materials (recorded on construction). The experimental results in Fig. 7 show the change in YR. Although the estimated strengths of the five degraded steels increased or decreased from those of fresh materials by various degradation mechanisms under different operating conditions, the yield ratio always increased with aging time. Considering the inverse relationship between the yield ratio and work-hardening exponent, the exponent value is expected to show a decreasing tendency. The extent of the change in the values may reflect operating and material conditions. Therefore, it is plausible that the yield ratio and work-hardening exponent proposed as new degradation indicators in this study can be properly applied to in-field facilities and structures. Continuing researches to extend the types of materials and to establish the engineering procedure for detailed in-field application are currently under way.

4. Conclusions

An instrumented indentation technique was applied to determine new mechanical parameters that can be obtained non-destructively in industrial fields. From lab-scale tests, both the work-hardening exponent and yield ratio were found more useful as general degradation indicators than hardness and yield/tensile strengths. In-field applicability of these parameters was in part verified through in-field indentation tests.

References

[1] J.-H. Ahn, D. Kwon, J. Mater. Res. 16 (2001) 3170–3178.
[2] E.-C. Jeon, J.S. Park, D. Kwon, Trans. ASME J. Eng. Mater. Tech. 125 (2003) 406–411.
[3] K.L. Murty, P.Q. Miraglia, M.D. Mathew, V.N. Shah, F.M. Haggag, Int. J. Pres. Ves. Pip. 76 (1999) 361–369.
[4] M.D. Mathew, K.L. Murty, K.B.S. Rao, S.L. Mannan, Mater. Sci. Eng. A264 (1999) 159–166.
[5] T. Yamamoto, H. Kurishita, T. Matsushima, H. Kayano, J. Nucl. Mater. 239 (1996) 219–227.
[6] D.G. Park, T.S. Byun, Y.Y. Song, J.H. Hong, I.S. Kim, Key Eng. Mater. 183-1 (2000) 607–612.
[7] W.C. Oliver, G.M. Pharr, J. Mater. Res. 7 (1992) 1564–1583.
[8] A.L. Norbury, T. Samuel, J. Iron Steel Inst. 117 (1928) 673–687.
[9] R. Hill, B. Storåkers, A. Zdunek, Proc. R. Soc. Lond. A423 (1989) 301–330.
[10] F.A. Francis, Trans. ASME J. Eng. Mater. Tech. 98 (1976) 272–281.
[11] D. Tabor, Hardness of Metals, Oxford University Press, Oxford, 1951, pp. 79–83.
[12] G.E. Dieter, Mechanical Metallurgy, McGraw-Hill, New York, 1981, pp. 283–292.

[13] S.K. Kim, Y.M. Kim, Y.J. Lim, N.J. Kim, Proceedings of the 15th Conference on Mechanical Behavior of Materials, Korea Institute of Metals and Materials, Korea, 2001, pp. 177–186.
[14] J.-i. Jang, Y. Choi, J.-S. Lee, Y.-H. Lee, D. Kwon, M. Gao, R. Kania, Int. J. Fracture 131 (2005) 15–34.
[15] K. Kimura, T. Matsuo, M. Kikuchi, R. Tanaka, Tetsu-to-Hagane 72 (1986) 474–481.
[16] T. Shoji, Time-Dependent Degradation and Life-Time Prediction, Realize Inc., Japan, 1994, pp. 37–48.
[17] T. Shoji, Time-Dependent Degradation and Life-Time Prediction, Realize Inc., Japan, 1994, pp. 118–124.
[18] Y. Kondo, Y. Sakurai, J. Namekata, M. Tanaka, F. Hangai, Tetsu-to-Hagane 76 (1990) 1195–1201.
[19] D. Yamasaki, I. Hirata, T. Morimoto, K. Ono, Tetsu-to-Hagane 65 (1979) 969–974.
[20] M. Toyoda, J. Jpn. Weld. Soc. 58 (1989) 485–490.